J Chem Crystallogr
DOI 10.1007/s10870-013-0422-1

ORIGINAL PAPER

Synthesis and Structural Characterization of the Mononuclear Cobalt(II) Complex: {5,5′-Dihydroxy-2,2′-[*o*-phenylene-bis(nitrilomethylene)]diphenolato}cobalt(II) Dihydrate

Alina Soroceanu · Sergiu Shova · Maria Cazacu · Iolanta Balan · Natalia Gorinchoy · Constantin Turta

Received: 20 July 2012 / Accepted: 17 April 2013

Abstract The Schiff base ligand $H_2L{\cdot}C_2H_5OH$ derived from the condensation reaction between *o*-phenylenediamine and 2,4-dihydroxybenzaldehyde as well as its mononuclear complex $[CoL]{\cdot}2H_2O$ have been synthesized and characterized by X-ray crystallography, IR, ^1H NMR and UV–Vis analyses, and density functional theory (DFT B3LYP) calculations. The Co^{II} ion has a slightly distorted square-planar coordination provided by tetradentate dianionic N_2O_2 ligand L^{2-}. The spin state of the complex was determined as being $S = 1/2$. On the basis of DFT calculations, the UV–Vis absorption bands of the ligand can be assigned to the $^1A_1 \rightarrow {}^1B_2$ (two) and $^1A_1 \rightarrow {}^1A_1$ transitions, while for complex they correspond to the $^2A_2 \rightarrow {}^2B_1$ (two) and $^2A_2 \rightarrow {}^2A_2$ ones.

Keywords Schiff base · Salophen · Co(II)–complex · DFT calculations

Introduction

Schiff bases, azomethines or imines, are among the most used ligands due to their easy preparation as well as ability to bind a variety of metal ions (Co, Mn, Cu, Ni, Fe, Cr, Zn, V, etc.) [1]. Different ligand classes were developed based on the condensation between salicylaldehyde derivatives with a variety of diamines [2]. Either aliphatic or aromatic diamines were used resulting in salen and salophen-type ligands, respectively. These are [N,N,O,O] tetradentate ligands [3] having four coordinating sites and two axial sites open to additional ligands [3, 4]. An important precursor for Schiff base ligands is phenylenediamine. There are a lot of reports in literature on the complexes of salophen-type ligands based on *o*-phenylenediamine with different metals [1, 5–7]. One of the most studied is Co(salophen) complex due to the known biological role of cobalt, its complexes with tetratendate Schiff base ligands being widely used to mimic cobalamin (B12) coenzymes, particularly as dioxygen carriers and oxygen activators [8, 9]. Cobalt complexes that can reversibly coordinate molecular oxygen have been studied extensively [10]. The Co(II)–salen complex is extremely sensitive to oxygen and, in the presence of an additional donor group, forms six coordinated octahedral cobalt(III) complexes, whereas, in the same conditions, the Co(II)–salophen complex shows a low tendency to increase its coordination number [11]. These compounds are also of interest in supramolecular synthesis [1] or as catalysts for a variety of reactions [12–14]. Thus, cobalt–salen and cobalt–salophen complexes are used as catalysts for oxygen reduction [10]. Co(II) complexes of Schiff bases derived from salicylaldehyde and *o*-phenylenediamine have been prepared and used in catalytic oxygenation of 2,6-di-*tert*-butylphenol leading to the formation of benzoquinone and diphenoquinone. It has

Electronic supplementary material The online version of this article (doi:10.1007/s10870-013-0422-1) contains supplementary material, which is available to authorized users.

A. Soroceanu · S. Shova · M. Cazacu (✉) · C. Turta
"Petru Poni" Institute of Macromolecular Chemistry, Aleea Gr. Ghica Voda 41A, 700487 Iasi, Romania
e-mail: mcazacu@icmpp.ro

S. Shova
Institute of Applied Physics of ASM, Academiei Str. 5, 2028 Chisinau, Republic of Moldova

I. Balan · N. Gorinchoy · C. Turta
Institute of Chemistry of ASM, Academiei Str. 3, 2028 Chisinau, Republic of Moldova

Published online: 09 May 2013

been proved that, in this process, the Co(II) complexes form reversible adducts with molecular oxygen [15].

Different from other articles reporting the Co complexes of the salophen-type ligands in general based on salycilaldehyde and *o*-phenylenediamine [15–17] or 2,4-dihydroxybenzaldehyde and other diamines [18–20], we prepared the Schiff base, $H_2L{\cdot}C_2H_5OH$ (**1**), derived from 2,4-dihydroxybenzaldehyde and *o*-phenylenediamine and its Co mononuclear complex, $[CoL]{\cdot}2H_2O$ (**2**). The obtained compounds were investigated by IR, ^1H NMR, UV–Vis spectroscopy, X-ray crystallography, and density functional theory (DFT B3LYP) calculations methods. The presence of the additional free OH groups in the resulted complex would permit its using in the subsequent reactions or could confer functionality to the supramolecular assemblies formed through vacant coordination site.

Experimental

Materials

Cobalt (II) acetate tetrahydrate, $Co(CH_3COO)_2{\cdot}4H_2O$, >99 %, was purchased from Sigma-Aldrich. 2,4-Dihydroxybenzaldehyde (Aldrich Chemistry), $(HO)_2C_6H_3CHO$, AR, 98 %, m.p. 135–137 °C. *o*-phenylenediamine, $C_6H_8N_2$, OPD, >98 %, m.p. 98–102 °C was purchased from Aldrich Chemistry.

Equipments

Fourier transform infrared (FT-IR) spectra were recorded using a Bruker Vertex 70 FT-IR spectrometer. Registrations were performed in the transmission mode in the range 400–4,000 cm^{-1} at room temperature with a resolution of 2 cm^{-1} and accumulation of 32 scans. The samples were incorporated in dry KBr and processed as pellets in order to be measured.

The proton magnetic resonance (^1H NMR) spectra were acquired in DMSO-d_6 at 25 °C with a Bruker Avance DRX 400 MHz spectrometer operating at 400.13 MHz for 1H. The spectrometer was equipped with a 5 mm four nuclei, direct detection z-gradient probehead. Chemical shifts are reported in ppm and are referenced to chloroform $\delta^1H = 7.26$ ppm.

UV–Vis absorption spectra were recorded on spectrophotometer Shimadzu UV-1700 in DMF solution using quartz cuvettes of 1 cm.

Magnetic properties of complex at room temperature were determined by NMR (Bruker Avance DRX 400 MHz spectrometer) measurement using the Evans method [21–23]. The indicator compound was *t*-butanol in DMSO. The "dopped" solution with known quantity of investigated substance was prepared in a capillary tube and shift difference was measured directly.

X-ray Crystallography

Crystallographic measurements for **1** and **2** were carried out at room temperature with an Oxford-Diffraction XCALIBUR E CCD diffractometer equipped with graphite-monochromated Mo $K\alpha$ radiation. The crystals were placed 40 mm from the CCD detector. The unit cell determination and data integration were carried out using the CrysAlis package of Oxford Diffraction [24]. All structures were solved by direct methods using SHELXS-97 [25] and refined by full-matrix least-squares on Fo^2 with SHELXL-97 [26] with anisotropic displacement parameters for non-hydrogen atoms. All H atoms attached to carbon were introduced in idealized positions ($d_{CH} = 0.96$ Å) using the riding model with their isotropic displacement parameters fixed at 120 % of their riding atom. Positional parameters of the water molecules and OH-groups were obtained from difference Fourier syntheses and verified by the geometric parameters of the corresponding hydrogen bonds. The main crystallographic data together with refinement details are summarized in Table 1.

CCDC-843942 and CCDC-843778 contain the supplementary crystallographic data for this contribution. These data can be obtained free of charge via www.ccdc.cam.ac.uk/conts/retrieving.html (or from the Cambridge Crystallographic Data Centre, 12 Union Road, Cambridge CB2 1EZ, UK; fax: (+44) 1223-336-033; or deposit@ccdc.ca.ac.uk).

Procedure

*Synthesis of 5,5′-dihydroxy-2,2′-[o-phenylenebis (nitrilomethylene)]diphenol, $H_2L{\cdot}C_2H_5OH$, (**1**)*

A solution of *o*-phenylenediamine (0.39 g, 2.83 mmol) in 5 mL methanol was added with stirring at room temperature to a solution consisting of 1.0 g (7.24 mmol) 2.4-dihydroxybenzaldehyde and 5 mL methanol. The mixture was heated for 2 h at 70°C, then was left to stand overnight at room temperature and finally the solvent was removed at rotavap. The remained solid was successively washed with methanol and diethyl ether and dried at 40°C in vacuum oven. The compound was dissolved in ethanol to form a solution of about 2.5 wt%, refluxed for about 30 min after which was cooled at room temperature and stored in freezer for 3 days when yellow crystals separated.

Yield 73 %. Elemental analysis: Calcd. for $C_{22}H_{22}N_2O_5$ (M_r 394.42 g mol^{-1}), %C 66.98; H 5.63; N 7.11. Found, % C 67.42; H 4.50; N 7.09.

IR spectrum (KBr pellet), cm^{-1}: 3,857vw, 3,842vw, 3,825vw, 3,754vw, 3,737vw, 3,679vw, 3,611vw, 3,434m, 2,922m, 2,853w, 1,721m, 1,627vs, 1,610vs, 1,574vs, 1,548m, 1,499s, 1,474m, 1,453m, 1,390w, 1,361m,

Table 1 Crystallographic data, details of data collection and structure refinement parameters for **1** and **2**

Compound	**1**	**2**
Empirical formula	$C_{22}H_{22}N_2O_5$	$C_{20}H_{18}CoN_2O_6$
Formula weight	394.42	441.29
Temperature (K)	200.00(14)	293
Crystal system	Triclinic	Monoclinic
Space group	$P\bar{1}$	*C2/c*
a (Å)	8.7910(7)	10.8502(7)
b (Å)	11.2617(10)	17.9074(8)
c (Å)	11.5549(10)	9.3012(5)
α (°)	116.095(9)	90
β (°)	99.706(7)	103.327(6)
γ (°)	101.121(7)	90
V (Å^3)	965.46(14)	1758.54(17)
D_{calc} (g cm^{-3})	1.357	1.667
Z	2	4
μ (mm^{-1})	0.097	1.020
Reflections collected/ unique	9374/3593 (R_{int} = 0.0482)	4141/2067 (R_{int} = 0.0637)
Data/restraints/ parameters	3593/0/263	2067/3/139
R_1^a, [$I > 2\sigma(I)$]	0.0791	0.0560
wR_2^b	0.1924	0.1466
GOF[c]	1.033	1.033
$\Delta\rho_{max}/\Delta\rho_{min}$, ($e$Å^{-3})	0.45/−0.36	0.381/−0.550

[a] $R_1 = \Sigma||F_o| - |F_c||/\Sigma|F_o|$

[b] $wR_2 = \{\Sigma[w\ (F_o^2 - F_c^2)^2]/\Sigma[w(F_o^2)^2]\}^{1/2}$

[c] GOF = $\{\Sigma[w(F_o^2 - F_c^2)^2]/(n - p)\}^{1/2}$; where *n* is the number of reflections and *p* is the total number of parameters refined

1,324m, 1,308m, 1,250s, 1,190s, 1,175m, 1,160s, 1,123s, 1,094m, 1,048m, 1,018w, 977m, 886w, 852m, 842m, 797m, 746m, 602vw, 545w, 531m, 520w, 503w, 488w, 472w, 445w, 428vw, 416vw.

^{1}H NMR (DMSO), *δ,* ppm: 6.29 (2H, d, 2.40 Hz, H-3), 6.40 (2H, dd, 8.40, 2.40 Hz. H-2), 7.33-7.40 (4H, m, H-4,5,6,7), 7.44 (2H, d, 8.40 Hz, H-1), 8.76 (2H, s, H-8), 10.27 (2H, s, OH), 13.40 (2H, s, OH); the peaks intensity ratio 2:2:4:1:1:1:1.

UV–Vis (DMF), λ_{max}, nm (ε, dm^3 mol^{-1} cm^{-1}): 287 (ε = 30084), 330 (ε = 38831), 372 (ε = 28042).

Synthesis of {5,5′-dihydroxy-2,2′-[o-phenylenebis (nitrilomethylene)]diphenolato}-cobalt(II), $CoL{\cdot}2H_2O$, (**2**)

0.15 g (0.38 mmol) of the H_2L was dissolved in a solvent mixture consisting in 6 mL ethanol, 4 mL methanol and 4 mL DMF. This solution was added over the other consisting in into solution of 0.15 g (0.60 mmol) $Co(CH_3COO)_2{\cdot}4H_2O$ in 6 mL ethanol and stirred for 10 min at room temperature. The clear solution was left until dark yellow prismatic crystals of good quality were formed in a few weeks. These were separated by filtration, washed with methanol, dried and analyzed.

Yield 65 %. Elemental analysis: Calcd. for $C_{20}H_{18}N_2O_6Co$ (M_r 441.30 g mol^{-1}), % C 54.43; H 4.11; N 6.34. Found, % C 54.21; H 4.02; N 6.15.

IR spectrum (KBr pellet), cm^{-1}: 3,541w, 3,064vw, 2,921w, 1,655m, 1,603vs ν(C = N), 1,580vs, 1,554s ν(aromatic ring), 1,494m, 1,476m, 1,447s ν(CH_2), 1,382m, 1,368s, 1,299w, 1,283w, 1,245s, 1,237s, 1,204s, 1,191s, 1,156w, 1,120s, 1,044w, 992w, 973w, 903vw, 851m, 842m, 793m, 762m, 748w, 732w, 654w, 645w, 532w, 495m, 461vw.

^{1}H NMR spectrum: capillary filled with solution of 6.7 mg of cobalt complex, 0.030 mL DMSO-d_6, and 0.970 mL *t*-butanol was placed in the measuring NMR spectra tube containing the same mixture without compound under study. Two bands assigned to the protons of *t*-butanol were observed in NMR spectrum at 478.956 Hz (1.197 ppm) and 448.706 Hz (1.121 ppm) corresponding to the *t*-butanol from capillary and HMR tube, respectively.

UV–Vis (DMF), λ_{max}, nm (ε, dm^{3}mol^{-1}cm^{-1}): 322 (ε = 19800), 346 (ε = 18000), 394 (ε = 22800).

Results and Discussion

Two-step procedure was approached to prepare a Co(salophen) type complex. First, the compound **1** was prepared by reaction between *o*-phenylendiamine and 2,4-dydroxybenzaldehyde, in 1:2 molar ratio, in refluxing methanol. The formation of azomethine was proved by the presence in FTIR spectrum of the characteristic band at 1,627 cm^{-1} besides to other specific bands such as 3,066 cm^{-1} (aromatic C–H stretch), 1,610 and 1,574 cm^{-1} (aromatic ring vibrations), and 1,250 cm^{-1} (phenolic C–O stretch) (Fig. 1S). In ^{1}H NMR, the peak of the proton from azomethine (CH=N) group is present at 8.76 ppm besides to the peaks for OH at 10.26 and 13.40 ppm as well as aromatics in the range 6.29–7.40 in the ratio corresponding to the presumed structure (Fig. 1).

The obtained ligand was treated with a cobalt salt, $Co(CH_3COO)_2{\cdot}4H_2O$ forming the corresponding complex CoL (compound **2**). As a result of the complexation, the azomethine band in FTIR spectrum shifted from 1,627 cm^{-1} in free ligand to lower stretching frequency, 1,616 cm^{-1}, in complex. Bathochromic shifts are also recorded in the ν(phenolic C–O) band from 1250 in ligand at 1,237 cm^{-1} in complex that confirms the involving of oxygen in C–O–Co bond. The new found vibration bands at 495 and 645 cm^{-1} which are not present in the free Schiff base are attributed to the ν(phenolic O–Co) and ν(N–Co), respectively, due to the involvement of oxygen and nitrogen atoms in metal complexation [27].

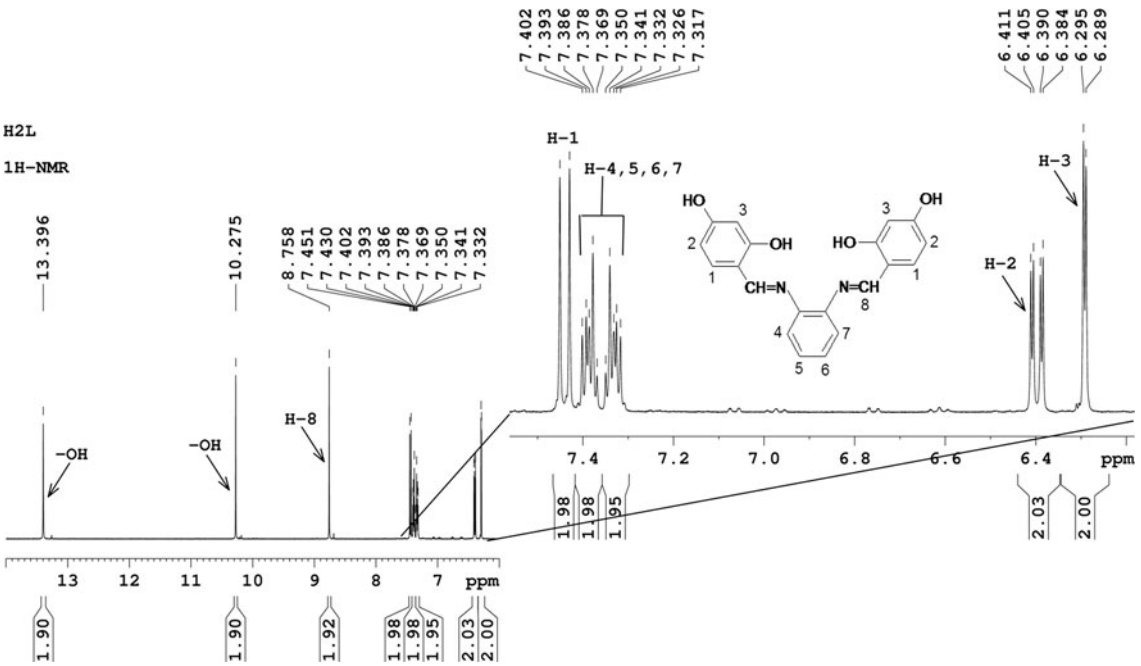

Fig. 1 ^{1}H NMR spectrum of the compound **1** (ligand H_2L) in DMSO-d_6

X-ray Crystallography

The X-ray structures of compounds **1** and **2**, along with atom-labelling schemes, are depicted in Figs. 2 and 4, respectively. Selected bond lengths and angles are summarized in Table 2.

The crystal **1** has a molecular structure built of the neutral molecules H_2L and ethanol as solvate molecules in 1:1 ratio associated via intermolecular H-bonds, where the OH-groups of the solvate molecules act as donor while the OH-group of the Schiff base as acceptor (Fig. 2). The conformation of the ligand molecule is stabilized through two intramolecular O–H···N H-bonds (Fig. 2). The H_2L molecule is essentially non-planar, because the aromatic ring denoted by C1–C6 atoms being twisted at N1-C8 bond, which arises from the intramolecular steric effect between two OH groups. The dihedral angle between two planar moieties is equal to 51.16(4)°. The main crystal packing motif of H_2L (**1**) is of zigzagging infinite chains packed parallel to *b* crystallographic axis (Fig. 3).

Each chain is built from the H_2L and solvate ethanol molecules linked via a system of H-bonds and π–π stacking interactions. One of the H-bond, which involves two of four hydroxyl groups with distances O3–H···O2(1 − *x*, 1 − *y*, 2 − *z*) = 1.82 Å, O3···O2′ = 2.619(4) Å and O3–H···O2′ angle of 165.2°, is responsible for the formation of centro-symmetric dimeric entities. Another two H-bonds: O4–H···O5(1 − *x*, − *y*,2 − *z*) = 1.83 Å, O4···O5′ = 2.649(4) Å, ∠O4–H···O5′ 173.7° and O5–H···O2 = 2.05 Å, O5···O2 = 2.814(4) Å, ∠O5–H···O2 151.3° sustain the formation of infinite chains. Secondary, there is face stacking of pairs of H_2L molecules, which is evidenced by the

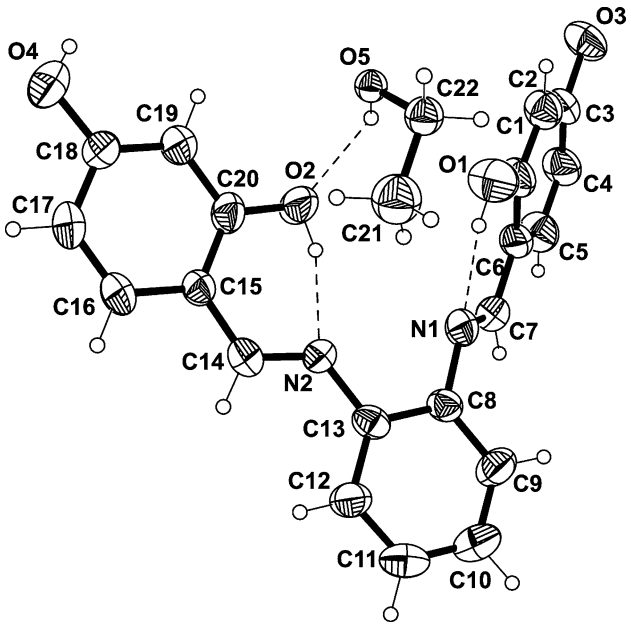

Fig. 2 X-ray structure of $H_2L{\cdot}C_2H_5OH$, **1** thermal ellipsoids are drawn at 40 % probability level. Intermolecular O5–H···O2 [O5–H 0.83 Å, H···O2 2.05 Å, O5···O2 2.814(4) Å, ∠O5–H···O2 151.3°] and two intramolecular hydrogen bonds O1–H···N1 [O1–H 0.82 Å, H···N1 1.91 Å, O1···N1 2.639(4) Å, ∠O1–H···N1 147.6°], O2–H···N2 [O1–H 0.85 Å, H···N1 1.92 Å, O1···N1 2.612(3) Å, ∠O1–H···N1 137.3° are also shown

centroid–centroid distance between centro-symmetrically related C1–C6 aromatic rings equal to 3.82 Å.

The Co atom in the crystal structure **2** occupies the special position on twofold axis; therefore the molecular structure of the CoL complex is characterized by imposed C_2 symmetry (Fig. 4). The central atom exhibits a slightly distorted N_2O_2 square-planar environment, provided by L^{2-} anion as a tetradentate ligand. The association of solvate water molecules with CoL complex occurs through H-bond, where the phenolic oxygen atoms act as acceptor (Fig. 4). The key role in crystal structure is played by O–H···O hydrogen bonds, which determine the formation of the double ribbons extending parallel to the *a* crystallographic axis (Fig. 5).

Table 2 Selected bond lengths (Å) and bond angles (°) for **1** and **2**

	1	2		1	2
Co1–O1	–	1.896(2)	C9–C10	1.371(5)	1.376(5)
Co1–N2	–	1.930(3)	C7–C6	1.442(5)	1.424(5)
N2–C7	–	1.295(4)	C6–C1	1.400(5)	1.422(5)
N2–C8	–	1.427(4)	C6–C5	1.395(5)	1.431(5)
N2–C13	1.417(4)	–	C5–C4	1.377(5)	1.351(5)
N2–C14	1.319(4)	–	C8–C9	1.390(5)	–
N1–C7	1.287(4)	–	C14–C15	1.397(5)	–
N1–C8	1.420(4)		C13–C12	1.382(4)	–
C8–C9	1.390(5)	1.373(4)	C12–C11	1.378(5)	–
O2–C3	–	1.356(4)	C11–C10	1.377(5)	–
O3–C3	1.350(4)	–	C13–C8	1.405(5)	–
O1–C1	1.355(4)	1.313(3)	C15–C20	1.440(5)	–
O4–C18	1.341(4)	–	C15–C16	1.417(5)	–
O2–C20	1.292(4)	–	C19–C18	1.378(5)	–
O5–C22	1.290(6)	–	C19–C20	1.397(5)	–
C2–C3	1.376(5)	1.380(4)	C17–C16	1.348(5)	–
C2–C1	1.368(5)	1.393(5)	C17–C18	1.406(5)	–
C3–C4	1.391(5)	1.392(5)	C21–C22	1.506(8)	–
O1–Co1–N1	–	94.9(1)	O1–Co1–N1′	–	172.3(1)
O1–Co1–O1′	–	86.4(3)	N1-Co1–N1′	–	84.9(2)

Symmetry code: ′) −x+1, y, −z+3/2

Magnetic Properties

The Eq. (1):

$$(\chi_i)_g = \frac{3}{4\pi m}\frac{\nu_0 - \nu_i}{\nu_0} + \chi_0, \quad (1)$$

where ν_0 is the frequency of the signal in the outer compartment, ν_i the frequency of the signal in the capillary (Fig. 2S), *m* the mass of paramagnetic substance in 1 mL of solution, χ_o is the gram susceptibility of solvent, and the experimental data obtained according to Evans method [21] were used to determine the effective magnetic moment of complex, μ_{eff}. A value of about 1.6 BM was obtained which means that the spin state of the complex S = 1/2 and its multiplicity is 2.

Electronic Structure

Both the ligand and the complex spectrum contain three UV–Vis absorption bands at 287, 330, 372 nm (**1**) and 322, 346, 394 nm (**2**), respectively (Fig. 6).

For assignment of these bands, the electronic structures of the ligand **1** and the complex **2** were calculated at the DFT B3LYP and Hartree–Fock CI levels. Quantum chemical calculations were performed using the PC GAMESS version [28] of the GAMESS (US) QC package

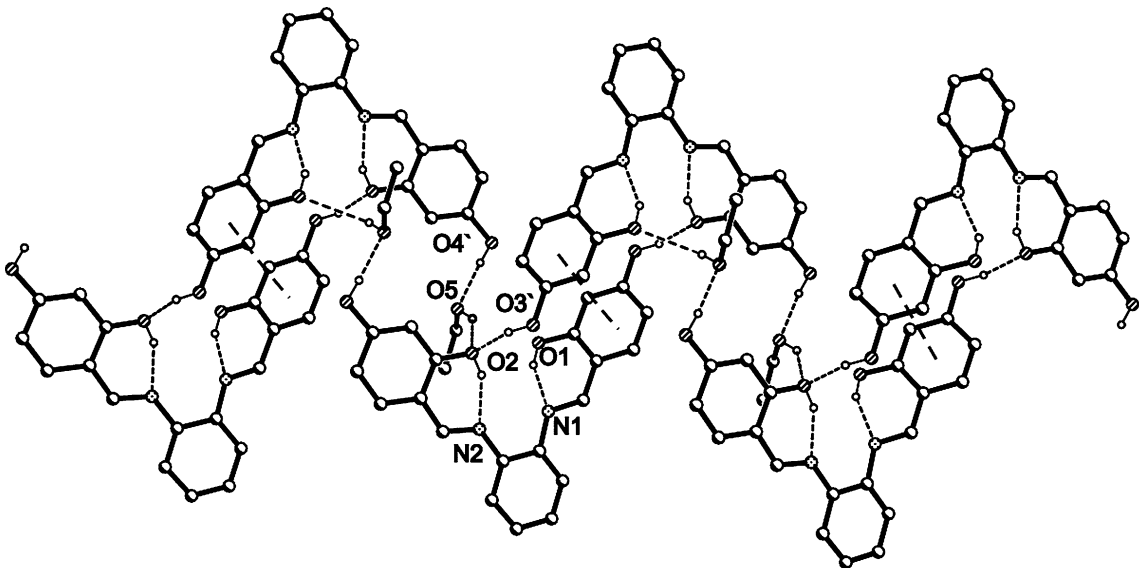

Fig. 3 View of the infinite chain in the crystal structure **1**

[29]. A full geometry optimization was carried out by means of all-electron spin-restricted DFT calculations employing the B3LYP hybrid functional [30, 31] in combination with the TZV basis set for all atoms [32, 33]. Electronic terms of excited states and electronic transition energies were obtained from single-point Hartree–Fock configuration interaction (CI) calculations at the optimized geometries. The CI matrices in both cases included all configurations produced by single and double excitations from the five highest occupied to five lower unoccupied MOs.

As a first step, the geometry optimization was carried out in the assumption that the spatial nuclear configuration of considered compounds corresponds to the C_{2v} point group of symmetry; the *z*-axis lies in the plane of the ligand and bisects the latter; the *x*-axis is perpendicular to the plane of the ligand. The basis for this choice was the experimental X-ray data, according to which the central atom exhibits a slightly distorted N_2O_2 square-planar environment in **2**. However, the vibration analysis of

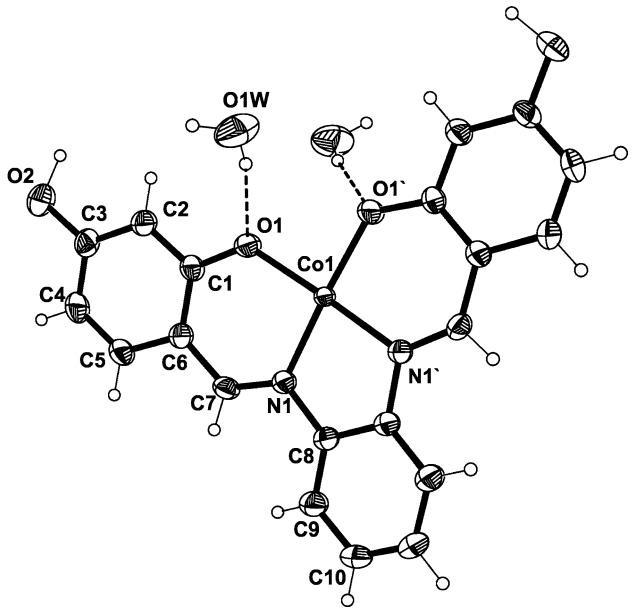

Fig. 4 X-ray structure of CoL·2H_2O, **2**. Thermal ellipsoids are drawn at 40 % probability level. H-bond parameters: O1*w*–H···O1 [O1*w*–H 0.86 Å, H···O1 1.95 Å, O1*w*···O1 2.796(4) Å, ∠O1*w*–H···O1 167.1°

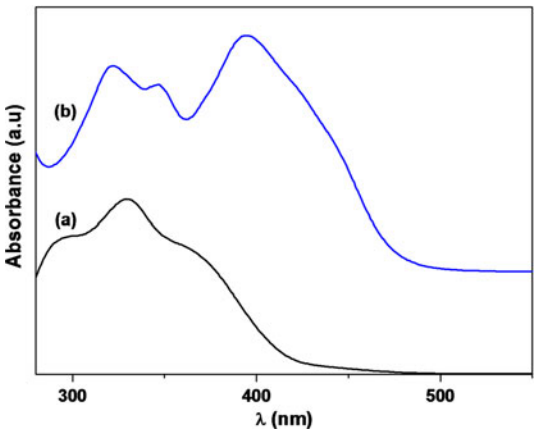

Fig. 6 UV–Vis spectra for: *a* compound **1** (ligand H_2L); *b* compound **2** (complex CoL) in DMF

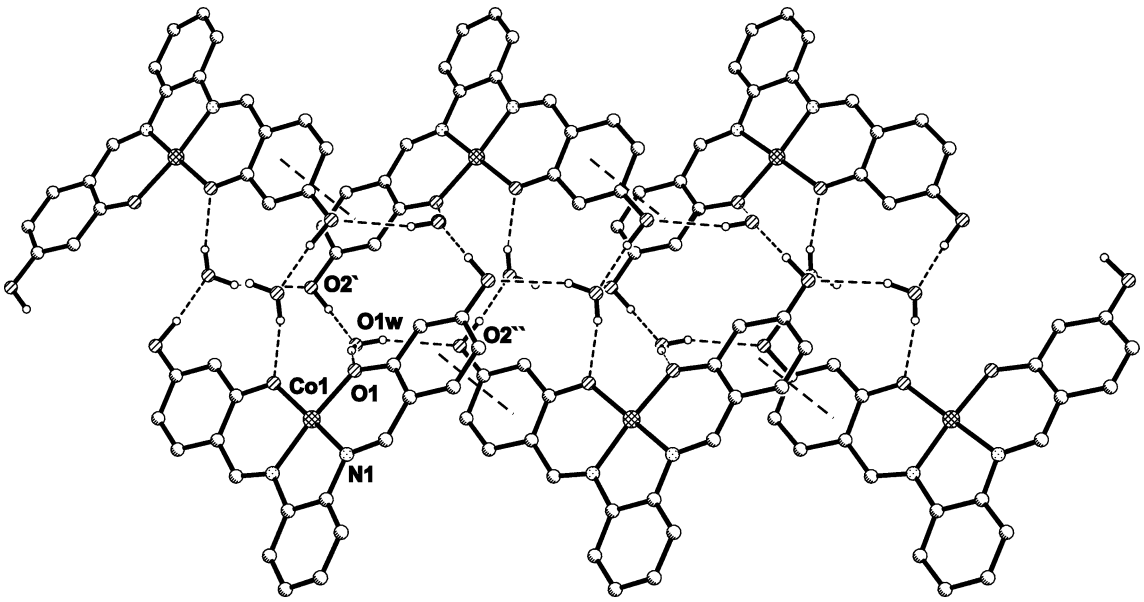

Fig. 5 The fragment of the crystal structure of CoL·2H_2O, 2. H-bond parameters: O2–H···O1*w* [O2–H 0.82 Å, H···O1*w*(1 − *x*, 1 − *y*, 1 − *z*) 1.90 Å, O2···O1*w*′ 2.720(4) Å, ∠O2–H···O1*w* 175.7°]; O1*w*–H···O2 [O1*w*–H 0.82 Å, H···O2(1 − *x* , + *y*, 0.5 − *z*) 2.37 Å, O1*w*···O2′ 3.181(4) Å, ∠O1*w*–H···O2 159.5°]

considered compounds in the C_{2v} symmetry shows the presence of one imaginary frequency corresponding to the out-of-plane distortion of the a_2 symmetry leading to the structures of C_2 symmetry. These are the twist of two peripheral phenyl rings around the N1–C8 and N2–C13 bonds (Fig. 2) in the ligand molecule **1**, and the "propeller" type distortion of N_2O_2 moiety around the atom of Co in the complex **2**. Optimized in C_2 symmetry structures of **1** and **2** correspond to the true minima with all real frequencies.

Table 3 Most important calculated and experimental distances (Å) and bond angles (°) in ligand **1** and complex **2**

1			**2**		
Geometry parameters	Calc.	Exp.	Geometry parameters	Calc.	Exp.
O1–H	1.024 (0.63)[a]	0.82	Co1–N2	1.909 (0.415)[a]	1.930
N1···H1	1.656 (0.17)[a]	1.91	Co1–O1	1.878 (0.457)[a]	1.896
N1···O1	2.57	2.639	O1–Co1–N1	93.8	94.9
N1–C8	1.41	1.420	O1–Co1–O1′	86.8	86.4
N1–C7	1.31	1.287	O1–Co1–N1′	176.9	172.3
O1–C1	1.358	1.355	N1–Co1–N1′	85.7	84.9
O1–H···N1	146.3	147.6			
dihedral	51.16	52.93			

[a] In parentheses is the value of the bond order

The most important bond distances and angles in optimized molecular structures are summarized in Table 3. As can be seen from Tables 2 and 3, the method used provides the structural values which are in a close agreement with the experimental ones. Note also that the calculations confirm the presence of intramolecular hydrogen bonds O–H···N in compound **1** (the value of the N–H bond order is approximately 0.2).

The molecular orbital diagrams for the frontier orbitals in compounds **1** and **2** are depicted in Figs. 7 and 8 together with the schemes of the electronic terms obtained from CI calculations at the optimized geometries. The energies and electronic configurations of the terms are given in Tables 4 and 5 together with the experimental data on the UV–Vis spectra.

As can be seen from Fig. 7 and Table 4, the low-lying excited states of the ligand **1** are formed by one-electron excitations from HOMO (b) and HOMO-1 (a) to the LUMO (a*) and LUMO + 1 (b*). These latter, in turn, are the π and π* molecular orbitals built up from the p_π-functions of the phenyl rings and the corresponding p_π-orbitals of the nitrogens and the oxygens. From the analysis of composition of these orbitals one can conclude that the $1^1A \rightarrow 2^1A$ excitation corresponds to a redistribution of the electron density within the central phenyl ring, whereas the other two $1^1A \rightarrow 1, 2\ ^1B$ excitations are accompanied by the electron charge transfer from the

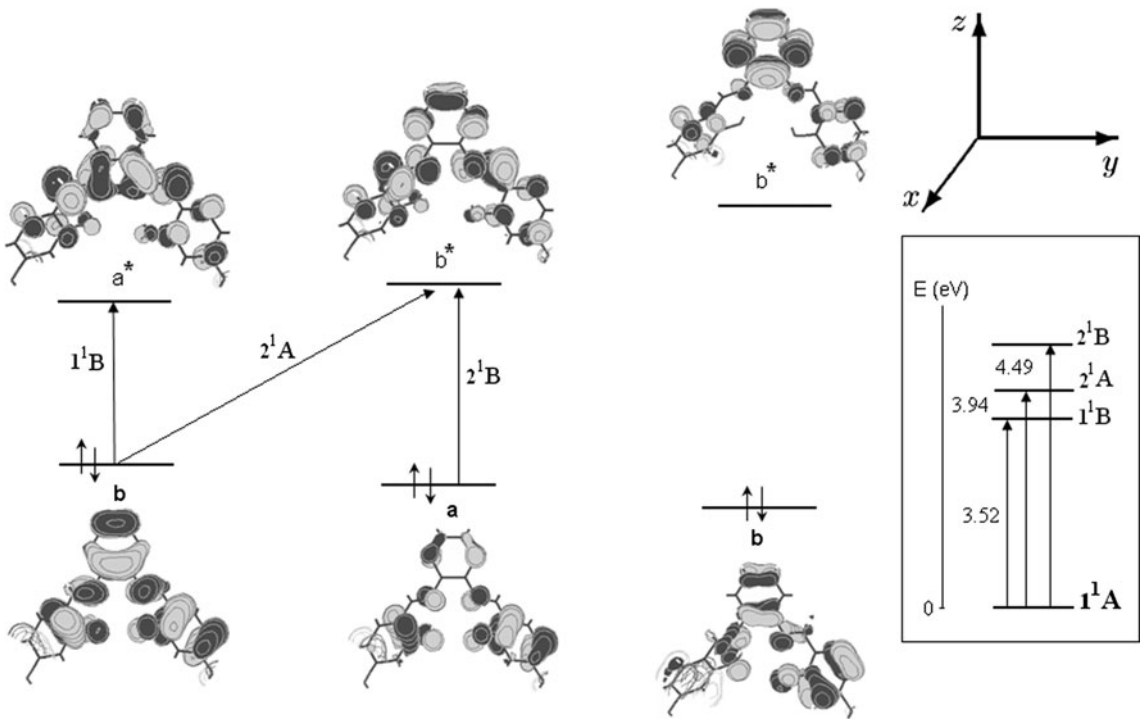

Fig. 7 Frontier molecular orbitals and electronic terms of the ligand **1**. The *arrows* on the MO diagram indicate the one-electron excitations that form corresponding excited states

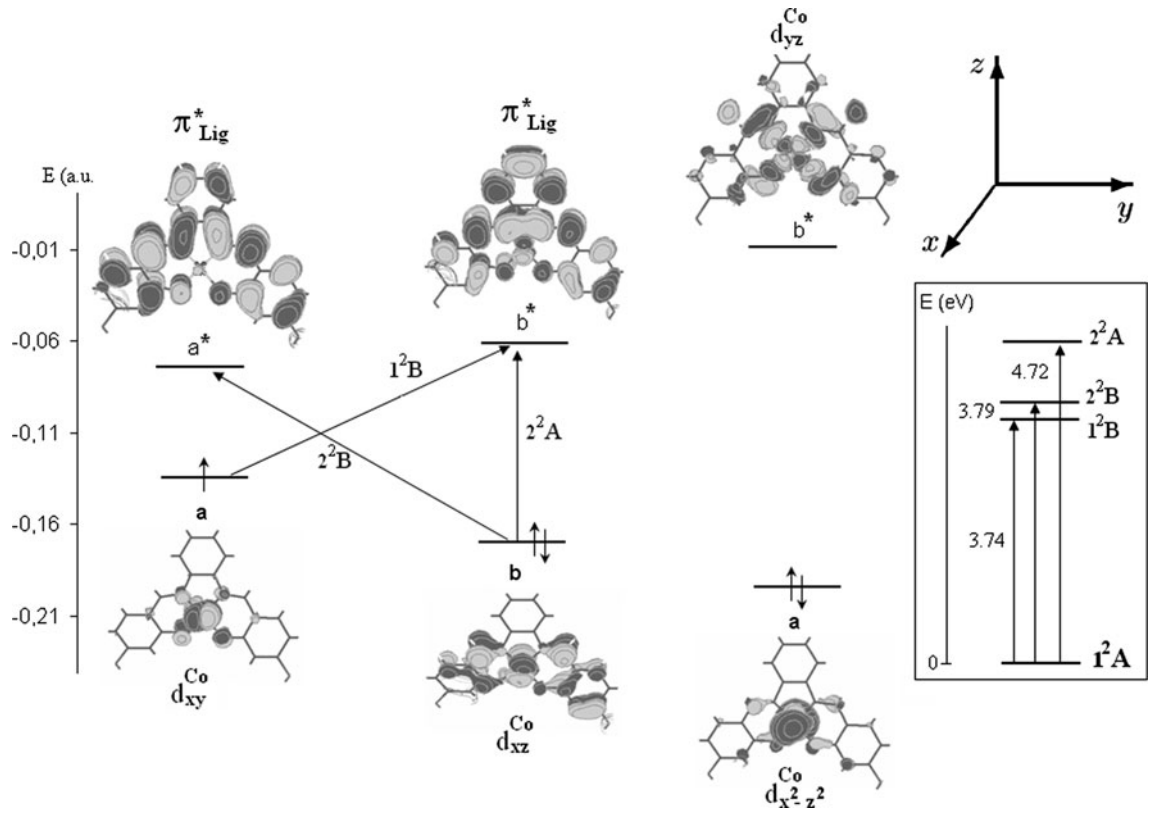

Fig. 8 Frontier molecular orbitals and electronic terms of **2**. The *arrows* on the MO diagram indicate the one-electron excitations that form the corresponding excited states. The nomenclature of 3d-AOs of Co is given in accordance with the coordinate system at the top right

peripheral rings on the central one. Table 4 shows a rather good agreement between calculated energies of the excited terms and the UV–Vis spectrum for **1**. Thus, the electronic absorption spectrum of this compound arises from $\pi \rightarrow \pi^*$ transitions and can be explained by considering the four frontier orbitals.

In the complex **2**, the three highest occupied molecular orbitals are composed mainly of 3d-orbitals of the metal: the weight of the $3d_{xy}$ AO of Co in the single-occupied HOMO (a) is at $\approx$92 %, the HOMO-1 (b) is the linear combination of the $3d_{xz}$ AO of Co ($\approx$70 %) and p_π AOs of peripheral rings ($\approx$30 %), and the HOMO-2 (*a*) is at 93 % the $3d_{x_2-z_2}$ AO of the metal. The two lowest unoccupied MOs (*a**) and (*b**) are the π^*-orbitals of the ligand (Fig. 8). The first excited state 1^2B of the complex **2** is obtained by one-electron excitation $a \rightarrow b^*$; its electronic configuration corresponds to one unpaired electron above the closed shell. This excitation is characterized by the electron density transfer from the metal to (mostly) the central ring of the ligand. The electronic configuration of other two excited states 2^2B ($b \rightarrow a^*$) and 2^2A ($b \rightarrow b^*$) corresponds to three unpaired electrons on three orbitals (Table 5). These two excitations, $1^2A_2 \rightarrow 2^2B$ and $1^2A_2 \rightarrow 2^2A$, are accompanied by the electron charge transfer both from metal and from the peripheral rings on the central ring of the ligand. As can be seen from the Table 5, the calculated energies of the excited states agree relatively well with the experimental data.

Table 4 Relative energies ΔE (e*V*) and electronic configurations of the ground and low-lying excited states for **1**

State	ΔE calc.	ΔE exp.	Electronic configuration
1^1A	0.00		$\{\ldots a^2\ b^2 \mid a^{*\,0}\ b^{*\,0}\ldots\}$
1^1B	3.52	3.33	$\{\ldots a^2\ b^1 \mid a^{*\,1}\ b^{*\,0}\ldots\}$
2^1A	3.94	3.76	$\{\ldots a^2\ b^1 \mid a^{*\,0}\ b^{*\,1}\ldots\}$
2^1B	4.49	4.32	$\{\ldots a^1\ b^2 \mid a^{*\,0}\ b^{*\,1}\ldots\}$

Table 5 Relative energies ΔE (e*V*) and electronic configurations of the ground and low-lying excited states for **2**

State	ΔE calc.	ΔE exp.	Electronic configuration
1^2A	0.00		$\{\ldots b^2\ a^1 \mid a^{*\,0}\ b^{*\,0}\ldots\}$
1^2B	3.74	3.15	$\{\ldots b^2\ a^0 \mid a^{*\,0}\ b^{*\,1}\ldots\}$
2^2B	3.79	3.58	$\{\ldots b^1\ a^1 \mid a^{*\,1}\ b^{*\,0}\ldots\}$
2^2A	4.72	3.85	$\{\ldots b^1\ a^1 \mid a^{*\,0}\ b^{*\,1}\ldots\}$

Conclusions

A Co(II)–complex of salophen type ligand was prepared by a two-steps procedure, including ligand preparation and its using in cobalt complexation. Both the ligand and the complex were isolated as crystals suitable for X-ray diffraction on a single crystal. The results correlate well with the spectral and analytical data. The calculated value of the effective magnetic moment of the complex, $\mu_{eff} \approx 1.6$ BM, as well as quantum-chemical calculations indicate that the spin state of the complex $S = 1/2$, and its multiplicity is 2. On the basis of quantum chemical calculations, one can conclude that the electronic absorption spectrum of the ligand arises from $\pi \rightarrow \pi^*$ transitions and can be explained within the four-orbital model. The absorption bands of the complex can be attributed to the electron density transfer from both the metal and the peripheral rings to the central ring of the ligand.

Acknowledgments This research was financially supported by European Regional Development Fund, Sectoral Operational Programme "Increase of Economic Competitiveness", Priority Axis 2 (SOP IEC-A2-O2.1.2-2009-2, ID 570, COD SMIS-CSNR: 12473, Contract 129/2010-POLISILMET).

References

1. Dalla Cort A, Gasparrini F, Lunazzi L, Mandolini L, Mazzanti A, Pasquini C, Pierini M, Rompietti R, Schiaffino L (2005) J Org Chem 70:8877
2. Clever G (2006) Synthesis and characterization of a metal–salen base pair for the assembly of programmed metal arrays inside the DNA double helix. PhD thesis, Fakultät für Chemie und Pharmazie der Ludwig-Maximilians Universität München, Bad Neuenahr
3. Cozzi PG (2004) Chem Soc Rev 33:410
4. Atwood DA, Harvey MJ (2001) Chem Rev 101:37
5. Bhattacharjee CR, Das G, Mondal P, Prasad SK, Rao DSS (2011) Eur J Inorg Chem 9:1418
6. Oliveira P, Machado A, Ramos AM, Fonseca IM, Braz Fernandes FM, Botelho Do Rego AM, Vitala J (2007) Catal Lett 114:192
7. Kleij AW, Tooke DM, Spek AL, Reek JNH (2005) Eur J Inorg Chem 4626
8. Zhang YL, Ruan WJ, Zhao XJ, Wang HG, Zhu ZA (2003) Polyhedron 22:1535
9. Leung ACW, MacLachlan MJ (2007) J Inorg Organomet Polym Mater 17:57
10. Ortiz B, Park SM (2000) Bull Korean Chem Soc 21:405
11. Vafazadeh R, Kashfi M (2007) Bull Korean Chem Soc 28:1227
12. El-Medani S, Ali OMA, Ramadan RM (2005) J Mol Struct 738:171
13. Jacobsen EN, Kakiuchi F, Konsler RG, Larrow JF, Tokunaga M (1997) Tetrahedron Lett 38:773
14. Nishinaga A, Yamato H, Abe T, Maruyama K, Matsuura T (1988) Tetrahedron Lett 29:6309
15. Pui A, Dobrota C, Mahy JP (2007) J Coord Chem 60:581
16. Nagajothi A, Kiruthika A, Chitra S, Parameswari K (2012) Int J Res Pharm Biomed Sci 3:1768
17. Fasina TM, Ogundele O, Ejiah FN, Dueke-Eze CU (2012) Intern J Biol Chem 6:24
18. Handa S, Gnanadesikan V, Matsunaga S, Shibasaki M (2007) J Am Chem Soc 129:4900
19. Chen Z, Morimoto H, Matsunaga S, Shibasaki M (2008) J Am Chem Soc 130:2170
20. Mihara H, Xu Y, Shepherd NE, Matsunaga S, Shibasaki M (2009) J Am Chem Soc 131:8384
21. Evans DF (1959) J Chem Soc 2003
22. Bertini I, Luchinat C, Patigi G (2002) Prog NMR Spectrosc 40:249
23. Berger S, Braun S (2004) In 200 and more NMR experiments. Willey-VCH, Weinheim, p 305
24. CrysAlis RED, Oxford Diffraction Ltd. (Version 1.171.34.76) (2003)
25. Sheldrick GM (1990) SHELXS-97, Program for crystal structure solution. University of Göttingen, Göttingen
26. Sheldrick GM (1997) SHELXL-97, Program for the refinement of crystal structures from diffraction data. University of Göttingen, Göttingen
27. Hamil AM, Khalifa KM, AL-Houni A, El-ajaily MM (2009) Rasayan J Chem 2:261
28. Granovsky AA. http://classic.chem.msu.su/gran/firefly/index.html. Accessed 12 Jan 2010
29. Schmidt MW, Baldridge KK (1993) J Comput Chem 14:1347
30. Becke AD (1993) J Phys Chem 98:5648
31. Lee C (1988) Phys Rev 37:785
32. McLean AD, Chandler GS (1980) J Chem Phys 72:5639
33. Schafer A, Huber C, Ahlrichs R (1994) J Chem Phys 100:5289